CHEMISTRY
AN ASIAN JOURNAL
ACES
FULL PAPER

DOI: 10.1002/asia.201400062

Ultrafast Dynamics of Solvation and Charge Transfer in a DNA-Based Biomaterial

Susobhan Choudhury,[a] Subrata Batabyal,[a] Tanumoy Mondol,[a] Dilip Sao,[a] Peter Lemmens,[b] and Samir Kumar Pal*[a]

Abstract: Charge migration along DNA molecules is a key factor for DNA-based devices in optoelectronics and biotechnology. The association of a significant amount of water molecules in DNA-based materials for the intactness of the DNA structure and their dynamic role in the charge-transfer (CT) dynamics is less documented in contemporary literature. In the present study, we have used a genomic DNA–cetyltrimethyl ammonium chloride (CTMA) complex, a technological important biomaterial, and Hoechest 33258 (H258), a well-known DNA minor groove binder, as fluorogenic probe for the dynamic solvation studies. The CT dynamics of CdSe/ZnS quantum dots (QDs; 5.2 nm) embedded in the as-prepared and swollen biomaterial have also been studied and correlated with that of the timescale of solvation. We have extended our studies on the temperature-dependent CT dynamics of QDs in a nanoenvironment of an anionic, sodium bis(2-ethylhexyl)-sulfosuccinate reverse micelle (AOT RMs), whereby the number of water molecules and their dynamics can be tuned in a controlled manner. A direct correlation of the dynamics of solvation and that of the CT in the nanoenvironments clearly suggests that the hydration barrier within the Arrhenius framework essentially dictates the charge-transfer dynamics.

Keywords: charge transfer · DNA · quantum dots · solvation dynamics · thin films

Introduction

A significant development of DNA-based materials in the field of nanophotonics and optoelectronics has been evident in recent years.[1–5] A class of DNA-based thin films is made of a genomic DNA–cationic surfactant (cetyltrimethyl ammonium chloride: CTMA) complex, which acts as an efficient electron-blocking layer (EBL)[6,7] in the development of bio-LEDs (light-emitting diodes). Remarkably, as evident from the circular dichroism (CD) spectroscopic studies,[8] DNA retains its physiological B-form in the thin film. To unravel the role of DNA in thin films for electronics applications, the exploration of the charge-transfer (CT) mechanism of DNA in the thin film is unavoidable. In a series of earlier studies, it has been suggested that π–π interaction between base-pair stacking of double-stranded DNA could be responsible for the one-dimensional CT along the DNA chain.[9] The CT mechanism in the DNA matrix and classification of the matrix in insulators,[8] semiconductors,[10] conductors,[11] or even superconductors[12] invited several debates in the early and recent literature.[13] A significant portion of the experimental evidence, including the lack of anisotropy of conduction in the spun-fiber sample, suggests that the mechanism is not consistent with the one-dimensional "molecular-wire"-type charge transport within the base-pair core, but rather rapid charge migration in the outer mantle of the B-DNA superstructure.[9]

It has long been reported that the equilibrium structure, structural integrity, and biochemical function of a DNA duplex are strongly dependent on the degree of DNA hydration.[14] High-resolution X-ray crystallographic analysis,[15–17] neutron diffraction measurement,[14] and solution NMR spectroscopic study[18] of the B-form DNA revealed that the 'spine of hydration' exists in the narrow minor groove of physiologically active DNA. One of the previous studies suggests that decreasing humidity triggers the structural transition of DNA from the B to Z form owing to the volatilization of bound water molecules.[8] The role of water in the structural integrity of DNA is important because phosphate–phosphate electrostatic repulsion[19] is diminished by the high dielectric constant of water. In addition to the very existence of such water molecules in the DNA structure, the dynamics of these water molecules also play a pivotal role in maintaining the DNA structure and functionality.[20,21] The observation of the existence of water molecules within the DNA–CTMA film during thermogravimetric

[a] S. Choudhury, S. Batabyal, Dr. T. Mondol, D. Sao, Prof. Dr. S. K. Pal
Department of Chemical, Biological and Macromolecular Sciences
S. N. Bose National Centre for Basic Sciences
Block JD, Sector III, SaltLake, Kolkata 700 098 (India)
E-mail: skpal@bose.res.in

[b] P. Lemmens
Institute for Condensed Matter Physics, TU Braunschweig
Mendelssohnstrasse 3, 38106 Braunschweig (Germany)

Supporting information for this article is available on the WWW under http://dx.doi.org/10.1002/asia.201400062. It includes fluorescence measurement data of H258 in the as-prepared and swelled DNA–CTMA thin films (Tables S1 and S2) and the solvation relaxation of C-500 in AOT reverse micelles as mentioned in the text (Figures S1 and S2).

analysis (TGA) studies[8] probably points to the intactness of the B-form DNA in the DNA–CTMA film given the widely accepted fact that water is an integral part of biomolecular systems.[22–26]

The timescale related to charge migration in the DNA moiety is found to be ultrafast and ranges from a few picoseconds to several tens of nanoseconds.[27–29] To participate in the CT processes, the water molecules in the close vicinity of the DNA molecule (water of hydration) are expected to offer a similar solvation timescale. A series of ultrafast spectroscopic investigations reveal solvation timescales of the hydration water on similar orders.[28] Although the DNA–CTMA material is frequently used in optoelectronics and has been found to be a promising material for future technology,[4,6] surprisingly, the role of the water molecules in the material is absent in contemporary literature.[30] The dependence of device performance on the dynamics of the integrated water molecule within the DNA thin film is also sparsely documented in literature, and this is the motive of our present study.

Here, we have prepared DNA–CTMA thin films, generally used in designing bio-LEDs[7,31] by following the procedure reported elsewhere.[8] A well-characterized DNA minor groove binder dye, Hoechst 33258 (H258),[32,33] was used as a doping probe for spectroscopic investigation of the material. A detailed characterization that involved CD, FTIR, UV/Vis absorption, and steady-state fluorescence spectroscopy was used to confirm the structural integrity of the DNA molecule and localization of the probe H258 in the DNA minor groove in the biomaterial. Our picosecond-resolved time-correlated single-photon-counting (TCSPC) technique reveals the timescale associated with the solvation of the water molecules in the vicinity of DNA in the as-prepared material and after swelling. We have also investigated the ultrafast CT dynamics from embedded CdSe/ZnS quantum dots (QDs) in the thin film (Scheme 1) and compared it with that in the swollen material. The steady-state and time-resolved quenching of a fluorescence probe (here the QDs) in a DNA matrix is well documented as the manifestation of CT from/to the probe in the matrix.[34,35] To investigate the role of water molecules in the CT processes of the embedded QDs within the material, we have also studied the CT dynamics of the QDs in anionic sodium bis(2-ethylhexyl)sulfosuccinate reverse micelles (AOT RMs), in which the degree of hydration (number of water molecules) and dynamics of water molecules[36,37] around the entrapped QDs can be tuned in a controlled manner. The temperature-dependent dynamic light scattering (DLS) and picosecond-resolved CT dynamics of the entrapped QDs in the RM clearly reveal the role of dynamics of the water molecules in the DNA materials. The studies are expected to have a profound effect on the key areas of research for developing superior biomaterials-based optoelectronic devices.

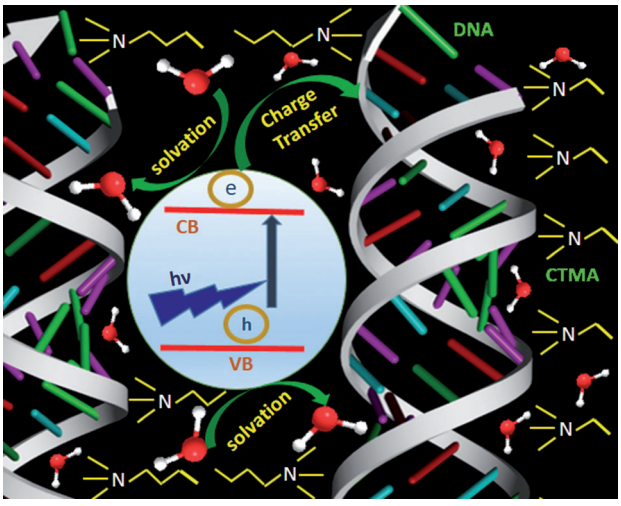

Scheme 1. Schematic representation of DNA–CTMA thin film. Embedded quantum dots (CdSe/ZnS) upon photoexcitation and charge transfer/solvation are also shown.

Results and Discussion

Figure 1 shows the absorption and emission spectra of as-prepared H258-doped and swollen DNA–CTMA thin film on a quartz plate (Scheme 1). Figure 1 also shows the corresponding spectra of the probe H258 in the aqueous solution. A slight redshift in the absorption spectra of H258 in the as-prepared and swollen thin films (355 nm) relative to the probe in buffer solution (347 nm) confirms the ground-state complexation of the probe in the minor groove of the DNA

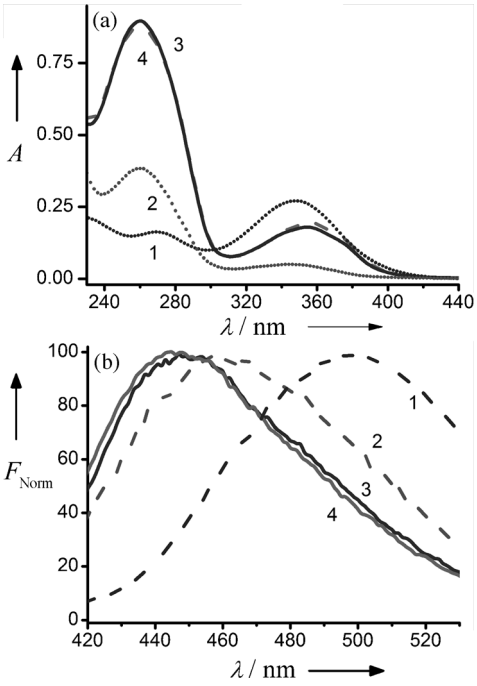

Figure 1. a) Absorption spectra of H258 in 1) buffer, 2) DNA in buffer, 3) DNA–CTMA film, and 4) swollen DNA–CTMA film. b) Emission spectra of H258 in 1) buffer, 2) DNA in buffer, 3) DNA–CTMA film, and 4) swollen DNA–CTMA film.

in the film.[38] A significant blueshift in the emission spectrum (at 447 nm) of the probe in the thin film with respect to that in aqueous buffer solution (at 460 nm) is also consistent with the location of the probe in the DNA minor groove (reported peak at 460 nm).[39] No significant difference between the absorption and emission spectra of the probe in the as-prepared and swollen film is consistent with the fact that the immediate environment of the minor groove binding probe H258 remains unperturbed in the presence of additional water molecules in the film. Figure 2a shows the CD spectra of the as-prepared and swollen films in which the positive peaks at 280 nm and negative peaks at 245 nm are the signature of the B-form DNA[40,41] in the films. The CD spectrum for the DNA in aqueous solution is also shown in Figure 2a as a reference. The structural integrity of the DNA (B-form) in the films with respect to that in the aqueous buffer solution is clearly evident from the figure. It has to be noted that the difference of the peak intensities of the films with respect to that in the DNA in aqueous buffer solution is due to the relatively lower concentration in the latter sample.

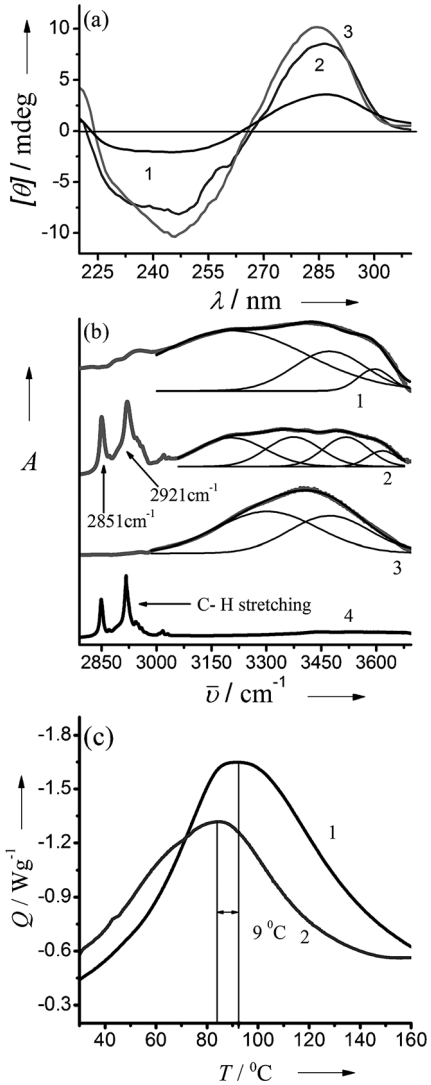

Figure 2. a) CD spectra of DNA in 1) buffer solution, 2) as-prepared DNA–CTMA thin film, and 2) swollen DNA–CTM thin film. b) FTIR spectra of 1) DNA fiber, 2) DNA–CTMA biomaterials, 3) bulk water, 4) and CTMA. To identify various types of water structures in the DNA and other systems, spectral deconvolution according to the Gaussian model was performed. c) DSC scan (10 °C min^{-1}) of 1) DNA and 2) DNA–CTMA complex. The endothermic maximum is due to the denaturation process of DNA.

To confirm the presence of strongly interacting water molecules in the film that lead to the monomeric form of the water,[42,43] we performed FTIR experiments, the results of which are shown in Figure 2b. The different C–H stretching modes of the DNA and the CTMA counterions (at 2851 and 2921 cm^{-1})[44] and O–H stretching frequencies of bulk water (at 3302 and 3472 cm^{-1}) are consistent with those reported in the literature.[45,46] In the case of DNA fiber without CTMA, the O–H stretching frequencies can be deconvoluted with essentially two peaks, in which one at 3468 cm^{-1} consistent with a bulk type and another at 3590 cm^{-1} corroborate the monomeric form of water molecules. The peak at 3204 cm^{-1} reveals an N–H stretching frequency in the DNA sample. In the case of the DNA–CTMA sample, the deconvoluted peaks at 3199 and 3607 cm^{-1} can be assigned to the stretching frequencies of N–H and monomeric water O–H, respectively. Two additional peaks at 3367 and 3508 cm^{-1} are similar to bulk-type water molecules in the sample.[47] Our FTIR studies reveal the existence of different types of water molecules in the biomaterial including strongly interacting (essentially associated to DNA–CTMA) water molecules in the material.

Additional evidence of the structural integrity of DNA in the biomaterial comes from thermometric studies of the films. In Figure 2c, differential scanning calorimetric (DSC) plots of DNA and the DNA–CTMA complex are shown in the temperature range from 30 to 160 °C. Endothermic maxima around 90 °C for DNA and the DNA–CTMA complex correspond to the melting of DNA. A closer look at the thermogram shows that the endothermic peak for the DNA–CTMA film is at least 9 °C lower than that of the pure DNA fiber. It has been reported earlier that the melting of the DNA molecule very much depends on the degree of hydration of the biomolecules.[48] The study that involves DNA melting in controlled humidity clearly showed that lower hydration leads to a relatively lower melting temperature of DNA. Thus our DSC study is consistent with the presence of water molecules in the biomaterial, yet they are lower in number than pure DNA fiber.

After confirmation of the structural integrity of DNA and the association of significant water molecules in the vicinity of DNA in the biomaterial, we investigated the dynamic timescales of the water molecules. Picosecond-resolved fluorescence transient of H258 bound to DNA in DNA–CTMA film (both as-prepared and swollen) have been measured at a number of wavelengths across the emission spectrum of H258 in the film, and the fluorescence lifetime values are tabulated in Tables S1 and S2 in the Supporting Information. Figure 3a and b show the decay transient of as-prepared and swollen DNA–CTMA film at three characteristic wave-

lengths from the blue to the red end of the fluorescence spectrum (410, 460, and 530 nm). The fluorescence transient detected in the blue region (410 nm) of the fluorescence spectrum is characterized by a faster picosecond decay component. The fluorescence transients become slower as the detection wavelengths increase and reveal a rise component at 530 nm. The nature of the wavelength-dependent transients across the emission spectrum of the probe H258 in the DNA matrix signifies solvation stabilization of the probe in the DNA environments.[21,49] However, the increase becomes more prominent in the case of swollen DNA–CTMA film as shown in Figure 3a and b. Figure 3c and d show the constructed time-resolved emission spectra (TRES) of H258 with a spectral shift of 1486 and 1420 cm^{-1} for as-prepared and swollen biomaterial, respectively, in an 11 ns time window, which indicates that H258 is stabilized due to the solvation by the minor groove water molecules in the excited state.[28] The observed solvation correlation decay profiles with time for corresponding systems are shown in the inset of Figure 3a and b, thus revealing temporal excited-state energy relaxation of the fluorophore in the DNA environments. Two-component exponential decay fitting of the solvation correlation decay profile of H258 bound to DNA in DNA–CTMA film (inset) yields time components of 0.235 (28%) and 8.83 ns (72%). For swollen DNA–CTMA film, the two time components were estimated to be 0.217 (29%) and 6.50 ns (71%), which are consistent with our previous studies on the solvation dynamics of DNA.[28,39] The longer components in both cases are due to the relaxation of DNA proper. The observation indicates that upon swelling some water molecules can access the DNA film, which allows the DNA molecule to become more flexible, thus leading to a faster stabilization of the probe H258 and results in a decrease in the time of water relaxation.

Table 1. The fluorescence lifetimes (τ_i) of QDs in as-prepared and swollen DNA–CTMA films.

System	τ_1 [ns] ([%])	τ_2 [ns] ([%])	τ_3 [ns] ([%])	τ_{avg} [ns]
QD film	–	1.78 (6)	13.16 (94)	12.48
QD-DNA film	0.06 (4)	1.52 (29)	6.04 (67)	4.49
swollen QD-DNA film	0.54 (8)	0.88 (40)	3.93 (52)	2.40

Table 2. Solvation correlation data for C-500 and the fluorescence lifetime (τ_i) data of QDs in AOT RM at different w_0 values.

	Solvation of C-500			QDs in RM				
w_0	τ_1 [ns] ([%])	τ_2 [ns] ([%])	τ_{sol} [ns]	τ_1 [ns] ([%])	τ_2 [ns] ([%])	τ_3 [ns] ([%])	τ_4 [ns] ([%])	τ_{avg} [ns]
0	–	–	–	0.84 (34)	10.8 (66)	–	–	7.4
2	0.34 (25)	4.13 (75)	3.18	0.12 (26)	0.84 (17)	2.36 (18)	10.8 (39)	4.80
4	0.29 (35)	2.68 (65)	1.83	0.09 (30)	0.84 (22)	3.32 (22)	10.8 (26)	3.69
8	0.19 (38)	1.59 (62)	1.06	0.09 (32)	0.84 (27)	3.78 (24)	10.8 (17)	2.98
12	0.16 (35)	1.49 (65)	1.03	0.01 (36)	0.84 (25)	3.70 (24)	10.8 (15)	2.77
20	0.13 (33)	1.35 (67)	0.95	0.11 (34)	0.84 (26)	3.65 (26)	10.8 (14)	2.69

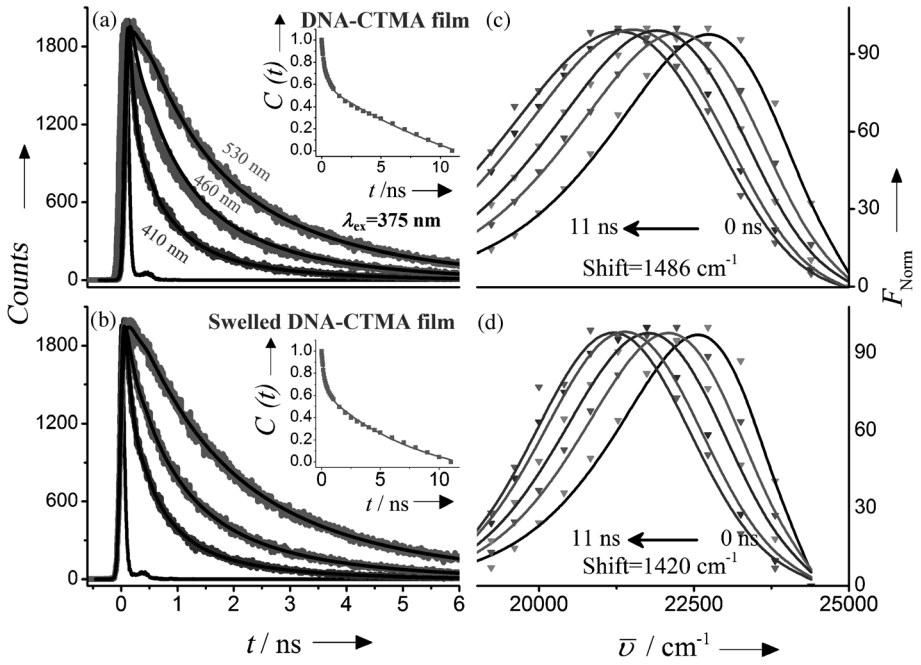

Figure 3. Picosecond-resolved transient of H258 at three different wavelengths in a) as-prepared DNA–CTMA and b) swollen DNA–CTMA biomaterial films. Values of λ_{em} are indicated. c,d) Time-resolved emission spectra (TRES) of corresponding systems are shown. Insets depict the corresponding solvation correlation decay profile of H258.

In a recent report, the effect of water molecules on the stabilization of the excited state of CdSe/ZnS QDs and the consequence of the water-molecule-stabilized state on the photoluminescence properties of the QDs has been reported.[50] In our studies we have used CdSe/ZnS QDs with a diameter of 5.2 nm as a CT probe in the DNA material. Figure 4a shows the steady-state fluorescence quenching of CdSe/ZnS QDs in the DNA matrix. The fluorescence of QDs in the matrix further quenches upon swelling of the film. The quenching of the excited-state lifetime of the QDs in the films before and after swelling is further confirmed by the picosecond-resolved fluorescence studies as shown in Figure 4b. The fluorescence lifetime of QDs in the quartz plate (with an average

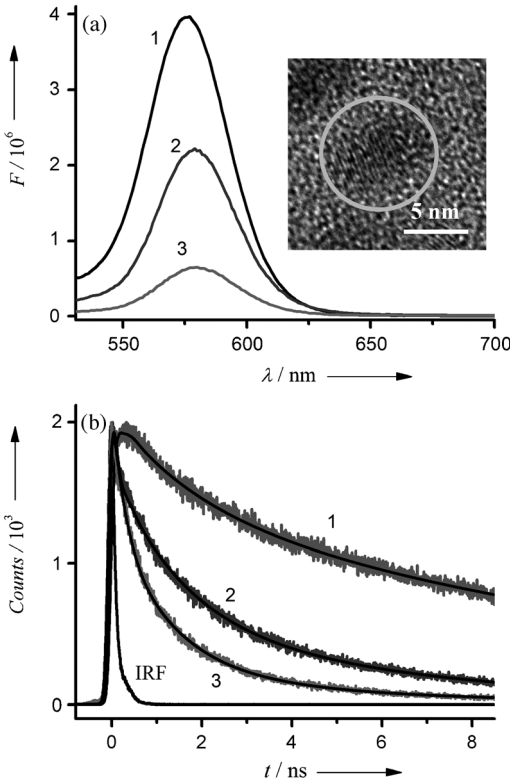

Figure 4. a) Fluorescence spectra of 1) CdSe/ZnS QDs, 2) QDs in as-prepared, and 3) swollen DNA–CTMA matrix ($\lambda_{ex}=510$ nm). b) Fluorescence decay transient of 1) QDs, 2) QDs in as-prepared, and 3) swollen DNA–CTMA matrix ($\lambda_{ex}=510$ nm and $\lambda_{em}=580$ nm).

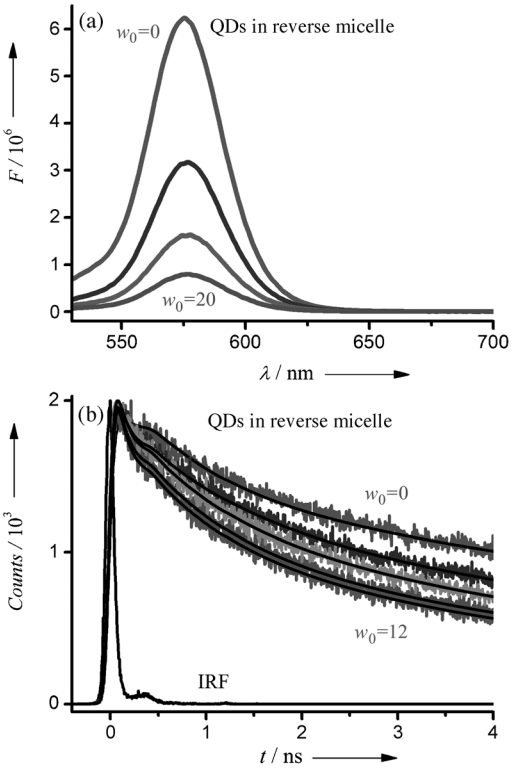

Figure 5. a) Steady-state fluorescence spectra of QDs in AOT RMs with increasing w_0 ($w_0=0$, 2, 4, and 20 with $\lambda_{ex}=510$ nm). b) Fluorescence decay transients of QDs in the AOT RMs at different w_0 values ($w_0=0$, 2, 4, 8, and 12 with $\lambda_{ex}=375$ nm and $\lambda_{em}=580$ nm).

lifetime 12.47 ns) becomes significantly faster in the as-prepared biomaterial (4.49 ns). Upon swelling of the film, the lifetime of QDs becomes even faster (2.40 ns). The details are tabulated in Table 1. The faster excited-state lifetime of the QDs in the biomaterial could be the manifestation of a photoinduced CT process from the embedded QDs to the DNA-bound water molecules in the matrix.[50] The apparent rate constants, k_{nr} (s), were determined for the excited-state nonradiative processes by comparing lifetimes of the QDs in the absence (τ_0) and in the presence (τ) of the DNA–CTMA complex by using the following equation [Eq. (1)]:[51,52]

$$k_{nr} = {}^{1}/_{\langle\tau\rangle} - {}^{1}/_{\langle\tau_0\rangle} \quad (1)$$

For the DNA–CTMA complex, the rate constant for the nonradiative process was found to be $1.4\times10^{8}\ s^{-1}$, whereas for the swollen system it is estimated to be $2.9\times10^{8}\ s^{-1}$, thus indicating a faster CT from QDs to the water molecules in the case of the swollen DNA–CTMA film.

To investigate conclusively the role of the dynamics of water molecules in the CT mechanism for QDs, we extended our studies with the model biomimetic, AOT RMs, whereby the number of water molecules (w_0) and the dynamics can be controlled (by tuning the temperature) precisely. Figure 5a shows that with an increase in water content ($w_0=2$ to 20) the fluorescence intensity of QDs entrapped in AOT RMs gradually decreases. The fluorescence decay transients of QDs in AOT RMs at different w_0 values are shown in Figure 5b. The faster excited-state lifetime of the QDs with increasing w_0 value from $w_0=0$ to 20 (water pool size from 1.6 to 9.6 nm) to reveal an average lifetime from 7.4 (at $w_0=0$) to 2.69 ns (at $w_0=20$, details are in Table 2) is evident from the figure. To determine a correlation between the dynamics of CT of the QDs in the RMs at various degrees of hydration (w_0) and the solvation dynamics of the RMs, we measured solvation correlation functions of the RMs using coumarin 500 (C-500) as fluorophore by following a procedure as reported previously[53] (Figures S1 and S2 in the Supporting Information). A linear correlation of the average solvation time constant (τ_s) and excited-state lifetime (τ_{avg}) of the QDs in the RMs up to $w_0=8$ is clearly evident from Figure 6a. It is well known that up to $w_0=8$, there is an insignificant possibility of bulk-type water, and all the water molecules are strongly interacting with the reverse micellar surface.[54,55] A further increase in the w_0 value begins to reveal two different types of water (bulk- and bound-type), and bulk-type water might cause permanent and irreversible surface damage to reveal an irrecoverable fluorescence of the entrapped QDs.[50] The reversibility of the fluorescence (both steady-state and time-resolved) of the QDs in the RMs from $w_0=8$ to 2 has also been confirmed (Figure 6b and Table 3).

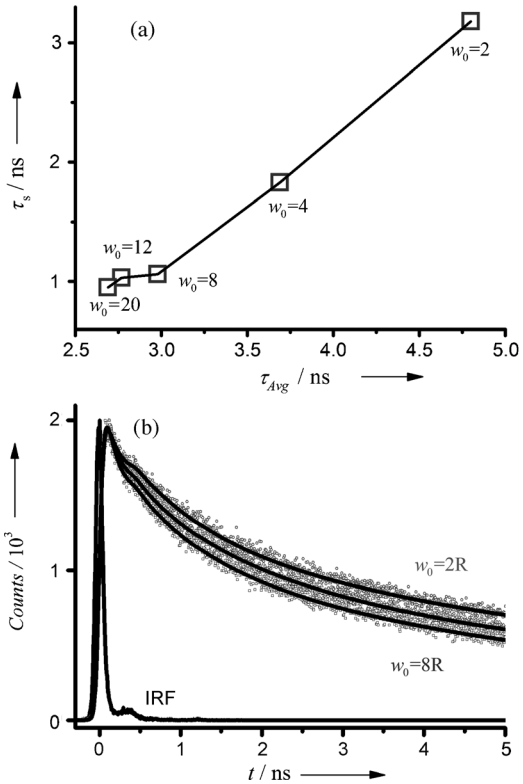

Figure 6. a) Plot of solvation time (τ_s) of C-500 probe against the average fluorescence lifetime (τ_{avg}) of the QDs at different w_0 values. b) Reversibility of fluorescence lifetime of QDs upon controlled reduction of RM size (w_0=8R, 4R, and 2R; R stands for reversible with λ_{ex}=375 nm and λ_{em}=580 nm).

Table 3. The fluorescence lifetimes (τ_i) of QDs in AOT RM at different w_0 values (R indicates reversible).

w_0	τ_1 [ns] ([%])	τ_2 [ns] ([%])	τ_3 [ns] ([%])	τ_4 [ns] ([%])	τ_{avg} [ns]
2R	0.11 (22)	0.84 (24)	2.41 (15)	10.8 (39)	4.78
4R	0.09 (27)	0.84 (28)	3.37 (16)	10.8 (29)	3.89
8R	0.01 (32)	0.84 (30)	3.74 (18)	10.8 (20)	3.07
12R	0.14 (30)	0.84 (24)	3.14 (22)	10.8 (24)	3.54
20R	0.12 (31)	0.84 (23)	3.20 (23)	10.8 (23)	3.42

Our observation of a faster rate of CT dynamics of QDs in the RMs of higher w_0 values and a distinct correlation with the solvation dynamics confirm the role of water molecules in the tuning of the CT rate in the nanoenvironments. However, the observation raises questions about the involvement of water molecules in the CT processes through dynamic flexibility of the water molecules or through the hydration number. To confirm the dynamic role of the water molecules in controlling CT processes, we studied the QDs in a particular RM with w_0=5 at various temperatures. As shown in Figure 7a, the DLS studies on the RM (w_0=5) with the QDs at different temperatures reveal an almost unaltered size of the RM and are consistent with our earlier observations.[53] However, the nonradiative rate of the CT dynamics of the QDs follows the Arrhenius law up to 60 °C (Figure 7b). Corresponding lifetime values are tabulated in

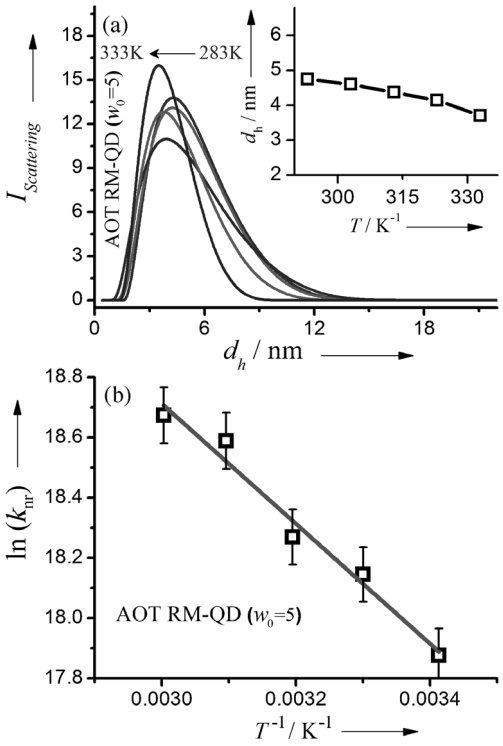

Figure 7. a) Typical DLS signals (scattering intensity) for w_0=5 AOT RM systems at different temperatures (293–333 K) are presented. The inset reveals hydrodynamic diameters (d_h) of reverse micelles for different temperatures. b) The Arrhenius plot of ln(k_{nr}) against 1/T for QDs in AOT RM with w_0=5 and its linear fit.

Table 4. The fluorescence lifetimes (τ_i) of QDs in AOT RM (w_0=5) at different temperatures.

T [K]	τ_1 [ns] ([%])	τ_2 [ns] ([%])	τ_3 [ns] ([%])	τ_{avg} [ns]
293	0.21 (31)	1.48 (30)	9.77 (39)	4.35
303	0.19 (31)	1.38 (31)	9.37 (38)	4.04
313	0.20 (33)	1.44 (31)	9.29 (36)	3.88
323	0.18 (36)	1.32 (30)	8.79 (34)	3.44
333	0.16 (35)	1.21 (31)	8.41 (34)	3.32

Table 4. The calculated barrier energy from the Arrhenius plot is 3.95 kcal mol^{-1}. Remarkably, it is noteworthy that the solvation barrier for this kind of RM (w_0=5) was estimated to be 2.4–4 kcal mol^{-1} from molecular dynamics simulation[56] and experimentally measured to be around 5 kcal mol^{-1}.[53] Our observation of the barrier-crossing-type CT reaction of the QDs in the RM and the similarity of the barrier with that of the solvation clearly unravel the role of the solvation barrier in the CT of the QDs in the RM.

Conclusion

In summary, we have investigated solvation dynamics of DNA-bound water in a technologically important biomaterial that consists of a DNA–CTMA self-assembly. The role the dynamics in the excited-state CT process of QDs-em-

bedded biomaterial has also been explored. Our studies on the solvation dynamics of water molecules in a controlled nanoenvironment of RMs and the CT of the QDs in that environment clearly reveal that the dynamic barrier (solvation) is the rate-limiting step for the CT process of the entrapped QDs. An interesting correlation of the dynamics of CT and solvation in the thin films (as-prepared and swollen) as well as in the RMs with different degrees of hydration up to $w_0 =$ 8 is evident from our studies. The solvation rate in the RMs of $w_0 = 2$ to 8 (swollen RMs) gradually increases from 3.1 to $9.4 \times 10^8\ s^{-1}$, respectively, thereby revealing the increase in the CT rate from 2.0 to $3.8 \times 10^8\ s^{-1}$. In the case of the DNA–CTMA thin film, the rate of solvation upon swelling increases from 1.6 to $2.1 \times 10^8\ s^{-1}$, and the corresponding increase in the CT rate is from 2.2 to $4.1 \times 10^8\ s^{-1}$, respectively. It is noteworthy that the dynamics of solvation and CT are essentially governed by the bound-type biological water,[26,49] and the increase in the CT rate with respect to that of the solvation in the case of RMs and the biomaterial upon swelling are found to be 4.5 and 3.8, respectively. The surprising correlation in both systems clearly justifies the role of biological water in the CT dynamics. Our finding might find relevance in QD-based devices in which one can effectively tune the efficiency by controlling the humidity level.

Experimental Section

Calf thymus DNA, potassium phosphate monobasic, and potassium hydroxide were obtained from Sigma and used without further purification. The fluorescent probe Hoechest 33258 (H258) and coumarin 500 (C-500) were purchased from Molecular Probes (99% purity) and Exciton, respectively. CTMA was a product of Aldrich. AOT was from Fluka (99% purity). The organic solvent *n*-butanol was purchased from Sisco Research Laboratories (spectroscopic grade). Isooctane was from Spectrochem. Birch yellow QDs, which is a suspension of CdSe QDs with a ZnS shell and TOPO capping, was purchased from Evidots (USA).

A 50 mM phosphate buffer (pH 7) was prepared by using potassium phosphate monobasic salt. An aqueous solution of DNA was prepared in phosphate buffer (50 mM). The DNA solution was sonicated to reduce the chain length of DNA. The H258-DNA solution was prepared by adding the requisite volume of probe solution (aqueous) to a DNA solution with a 20 mM base pair concentration so that final concentration of the probe was 2 mM with continuous stirring for 4–5 h. DNA–surfactant complexes were prepared according to the reported literature.[8] Briefly, drug-bound DNA aqueous solution was mixed with CTMA aqueous solution in a 1:1 stoichiometric combination, which led to a highly organized complex (Scheme 1). The insoluble complex was collected by filtration, washed with distilled water, and was then lyophilized to form freeze-dried powder. To avoid the adsorption of air moisture, the white powders of DNA–CTMA complexes were kept in a desiccator. The powder was dissolved in *n*-butanol, and the solution was uniformly spread on a quartz plate to prepare the thin film. The 'swollen DNA–CTMA film' was prepared by soaking the film under water for 30 min and finally removing the excess amount of surface water. The incorporation of QDs into the thin film was carried out by adding the QDs in butanol prior to dissolving the DNA–CTMA matrix into the butanol solution and thereafter following the same procedure as described above. AOT was dissolved in isooctane to a concentration of 100 mM, and then the calculated amount of water was injected into the solution to prepare the RMs of desired hydration, w_0, which is defined as relative molar concentration of water with respect to that of surfactant in the AOT RMs. Details of the RM synthesis and characterization have been published elsewhere.[53]

Since the DNA–CTMA film was transparent, steady-state fluorescence and absorption measurements were carried out with a Jobin–Yvon Fluorolog fluorimeter and a Shimadzu UV- spectrometer, respectively. A JASCO 815 spectrometer was used to study the circular dichroism (CD) spectra. For FTIR study, a JASCO FTIR-6300 instrument of 0.5 cm^{-1} resolution was used. Differential scanning calorimetry (DSC) data were obtained with a DSC-Q2000 from TA Instruments purging 100% N_2 at a heating rate of 10 °C min^{-1} in the temperature range from 30 to 160 °C. Above the temperature window, the sample was reported to be pyrolyzed and the sample became darkened.[48] Picosecond-resolved fluorescence decay transients were measured with a commercially available spectrophotometer (Life Spec-ps, Edinburgh Instruments, UK) with 70 ps instrument response function (IRF). The excitation at 375 and 510 nm was obtained with a pulse laser diode from PicoQuant, Germany. The observed fluorescence transients were fitted by using a nonlinear least-square fitting procedure to a function $(X(t) = \int_0^t E(t')R(t-t')dt')$ that consists of convolution of the IRF $(E(t))$ with a sum of exponential $(R(t) = A + \sum_{i=1}^{N} B_i e^{-t/\tau_i})$ with pre-exponential factors (B_i), characteristic lifetimes (τ_i), and a background (A). Relative concentration in a multiexponential decay was finally expressed as: $c_n = \frac{B_n}{\sum_{i=1}^{N} B_i} \times 100$. The quality of the curve fitting was evaluated by reduced chi-square and residual data. It should be noted that with our time-resolved instrument we were able to resolve at least one-fourth of the instrument response-time constants after the deconvolution of the IRF. The average lifetime (amplitude-weighted) of a multiexponential decay is expressed as: $\tau_{av} = \sum_{i=1}^{N} c_i \tau_i$. A time-resolved emission spectrum (TRES)[57] was used to construct time-dependent fluorescence Stokes shifts. The time-dependent fluorescence Stokes shifts, as estimated from TRES, were used to construct the normalized spectral shift correlation function or the solvent correlation function, $C(t)$, defined as, $C(t) = \frac{\nu(t)-\nu(\infty)}{\nu(0)-\nu(\infty)}$, for which $\nu(0)$, $\nu(t)$, and $\nu(\infty)$ are the emission maxima [cm^{-1}] at time 0, t, and ∞, respectively. The $\nu(\infty)$ value corresponds to the emission frequency beyond which an insignificant or no spectral shift is observed. The $C(t)$ function represents the temporal response of the solvent relaxation process. Dynamic light scattering (DLS) measurements were performed with a NanoS Malvern instrument that contained a 4 mW He:Ne laser ($\lambda = 632.8$ nm) equipped with a thermostatted sample chamber. All the scattered photons were collected at a 173° scattering angle. The scattering intensity data were calculated using the instrumental software to obtain the hydrodynamic diameter (d_h) and size distribution of the scatterer in each sample. The instrument measures the time-dependent fluctuation in the intensity of light scattered from the particles in solution at a fixed scattering angle. The hydrodynamic diameter (d_h) of the reverse micelles was estimated from the intensity autocorrelation function of the time-dependent fluctuation in intensity. The value d_h is defined as $d_h = \frac{k_b T}{3\pi\eta D}$, in which k_b is the Boltzmann constant, η is the viscosity, and D is the translational diffusion coefficient. In a typical size-distribution graph from the DLS measurement, the x axis shows a distribution of size classes in nanometers, whereas the y axis shows the relative intensity of the scattered light.

Acknowledgements

S.C. and S.B. thank the CSIR, India for the research fellowships. We thank DST (India) for financial grants (SB/S1/PC-011/2013 and DST/TM/SERI/2k11/103).

[1] N. C. Seeman, *Nature* **2003**, *421*, 427–431.
[2] Y. W. Kwon, C. H. Lee, D. H. Choi, J. I. Jin, *J. Mater. Chem.* **2009**, *19*, 1353–1380.
[3] P. V. Kamat, *J. Phys. Chem. C* **2008**, *112*, 18737–18753.
[4] A. J. Steckl, *Nat. Photonics* **2007**, *1*, 3–5.

[5] T. Singh, N. Sariciftci, J. Grote in *Org. Electron.*, *Vol. 223* (Eds.: T. Grasser, G. Meller, L. Li), Springer, Berlin, **2010**, pp. 73–112.
[6] Q. Sun, G. Subramanyam, L. Dai, M. Check, A. Campbell, R. Naik, J. Grote, Y. Wang, *ACS Nano* **2009**, *3*, 737–743.
[7] Q. Sun, D. W. Chang, L. Dai, J. Grote, R. Naik, *Appl. Phys. Lett.* **2008**, *92*, 251108–251110.
[8] L. Wang, J. Yoshida, N. Ogata, S. Sasaki, T. Kajiyama, *Chem. Mater.* **2001**, *13*, 1273–1281.
[9] J. M. Warman, M. P. de Haas, A. Rupprecht, *Chem. Phys. Lett.* **1996**, *249*, 319–322.
[10] Y.-G. Yang, P.-G. Yin, X.-Q. Li, Y. Yan, *Appl. Phys. Lett.* **2005**, *86*, 203901–203903.
[11] H. W. Fink, C. Schonenberger, *Nature* **1999**, *398*, 407–410.
[12] A. Y. Kasumov, M. Kociak, S. Guéron, B. Reulet, V. T. Volkov, D. V. Klinov, H. Bouchiat, *Science* **2001**, *291*, 280–282.
[13] K. Kawai, H. Kodera, Y. Osakada, T. Majima, *Nat. Chem.* **2009**, *1*, 156–159.
[14] S. Arai, T. Chatake, T. Ohhara, K. Kurihara, I. Tanaka, N. Suzuki, Z. Fujimoto, H. Mizuno, N. Niimura, *Nucleic Acids Res.* **2005**, *33*, 3017–3024.
[15] H. R. Drew, R. E. Dickerson, *J. Mol. Biol.* **1981**, *151*, 535–556.
[16] X. Shui, L. McFail-Isom, G. G. Hu, L. D. Williams, *Biochemistry* **1998**, *37*, 8341–8355.
[17] V. Tereshko, G. Minasov, M. Egli, *J. Am. Chem. Soc.* **1999**, *121*, 3590–3595.
[18] E. Liepinsh, G. Otting, K. Wüthrich, *Nucleic Acids Res.* **1992**, *20*, 6549–6553.
[19] K. Range, E. Mayaan, L. J. Maher, D. M. York, *Nucleic Acids Res.* **2005**, *33*, 1257–1268.
[20] S. K. Pal, L. A. Zhao, A. H. Zewail, *Proc. Natl. Acad. Sci. USA* **2003**, *100*, 8113–8118.
[21] D. Banerjee, S. K. Pal, *J. Phys. Chem. A* **2008**, *112*, 7314–7320.
[22] M. Maroncelli, J. Macinnis, G. R. Fleming, *Science* **1989**, *243*, 1674–1681.
[23] R. Jimenez, G. R. Fleming, P. V. Kumar, M. Maroncelli, *Nature* **1994**, *369*, 471–473.
[24] N. Nandi, K. Bhattacharyya, B. Bagchi, *Chem. Rev.* **2000**, *100*, 2013–2046.
[25] L. Zhao, S. K. Pal, T. Xia, A. H. Zewail, *Angew. Chem. Int. Ed.* **2004**, *43*, 60–63; *Angew. Chem.* **2004**, *116*, 62–65.
[26] S. K. Pal, A. H. Zewail, *Chem. Rev.* **2004**, *104*, 2099–2124.
[27] E. W. Schlag, D.-Y. Yang, S.-Y. Sheu, H. L. Selzle, S. H. Lin, P. M. Rentzepis, *Proc. Natl. Acad. Sci. USA* **2000**, *97*, 9849–9854.
[28] D. Banerjee, S. K. Pal, *Chem. Phys. Lett.* **2006**, *432*, 257–262.
[29] S. Shankara Narayanan, S. S. Sinha, P. K. Verma, S. K. Pal, *Chem. Phys. Lett.* **2008**, *463*, 160–165.
[30] M. Wolter, M. Elstner, T. Kubař, *J. Chem. Phys.* **2013**, *139*, 125102–125111.
[31] J. A. Hagen, W. Li, A. J. Steckl, J. G. Grote, *Appl. Phys. Lett.* **2006**, *88*, 171109–171111.
[32] H. Görner, *Photochem. Photobiol.* **2001**, *73*, 339–348.
[33] G. Cosa, K. S. Focsaneanu, J. R. N. McLean, J. P. McNamee, J. C. Scaiano, *Photochem. Photobiol.* **2001**, *73*, 585–599.
[34] C. Wan, T. Xia, H.-C. Becker, A. H. Zewail, *Chem. Phys. Lett.* **2005**, *412*, 158–163.
[35] C. Z. Wan, T. Fiebig, O. Schiemann, J. K. Barton, A. H. Zewail, *Proc. Natl. Acad. Sci. USA* **2000**, *97*, 14052–14055.
[36] G. B. Behera, B. K. Mishra, P. K. Behera, M. Panda, *Adv. Colloid Interface Sci.* **1999**, *82*, 1–42.
[37] R. Mitra, S. Sinha, S. Pal, *J. Fluoresc.* **2008**, *18*, 423–432.
[38] A. Adhikary, V. Buschmann, C. Muller, M. Sauer, *Nucleic Acids Res.* **2003**, *31*, 2178–2186.
[39] S. Batabyal, T. Mondol, S. Choudhury, A. Mazumder, S. K. Pal, *Biochimie* **2013**, *95*, 2168–2176.
[40] J. Kypr, I. Kejnovská, D. Renčiuk, M. Vorlíčková, *Nucleic Acids Res.* **2009**, *37*, 1713–1725.
[41] R. Sarkar, S. K. Pal, *Biopolymers* **2006**, *83*, 675–686.
[42] T. L. Tso, E. K. C. Lee, *J. Phys. Chem.* **1985**, *89*, 1612–1618.
[43] S. S. Narayanan, S. S. Sinha, R. Sarkar, S. K. Pal, *Chem. Phys. Lett.* **2008**, *452*, 99–104.
[44] M. Yang, Ł. Szyc, T. Elsaesser, *J. Phys. Chem. B* **2011**, *115*, 1262–1267.
[45] H. MacDonald, B. Bedwell, E. Gulari, *Langmuir* **1986**, *2*, 704–708.
[46] T. K. Jain, M. Varshney, A. Maitra, *J. Phys. Chem.* **1989**, *93*, 7409–7416.
[47] T. Kawai, J. Umemura, T. Takenaka, M. Kodama, S. Seki, *J. Colloid Interface Sci.* **1985**, *103*, 56–61.
[48] S. L. Lee, P. G. Debenedetti, J. R. Errington, B. A. Pethica, D. J. Moore, *J. Phys. Chem. B* **2004**, *108*, 3098–3106.
[49] S. K. Pal, J. Peon, B. Bagchi, A. H. Zewail, *J. Phys. Chem. B* **2002**, *106*, 12376–12395.
[50] K. Pechstedt, T. Whittle, J. Baumberg, T. Melvin, *J. Phys. Chem. C* **2010**, *114*, 12069–12077.
[51] I. Robel, M. Kuno, P. V. Kamat, *J. Am. Chem. Soc.* **2007**, *129*, 4136–4137.
[52] A. Makhal, H. Yan, P. Lemmens, S. K. Pal, *J. Phys. Chem. C* **2010**, *114*, 627–632.
[53] R. K. Mitra, S. S. Sinha, S. K. Pal, *Langmuir* **2008**, *24*, 49–56.
[54] A. Goto, S. Harada, T. Fujita, Y. Miwa, H. Yoshioka, H. Kishimoto, *Langmuir* **1993**, *9*, 86–89.
[55] N. M. Correa, M. A. Biasutti, J. J. Silber, *J. Colloid Interface Sci.* **1995**, *172*, 71–76.
[56] S. Pal, S. Balasubramanian, B. Bagchi, *J. Phys. Chem. B* **2003**, *107*, 5194–5202.
[57] M. L. Horng, J. A. Gardecki, A. Papazyan, M. Maroncelli, *J. Phys. Chem.* **1995**, *99*, 17311–17337.

Received: January 13, 2014
Revised: February 19, 2014
Published online: March 24, 2014

